

# A Colloidal Route to Semiconducting Tungsten Disulfide Nanosheets with Monolayer Thickness – Supporting Information

*Gabriele Pippia,<sup>a</sup> Diem Van Hamme,<sup>a</sup> Beatriz Martin-Garcia,<sup>b</sup> Mirko Prato,<sup>c</sup> Iwan Moreels.\*<sup>a</sup>*

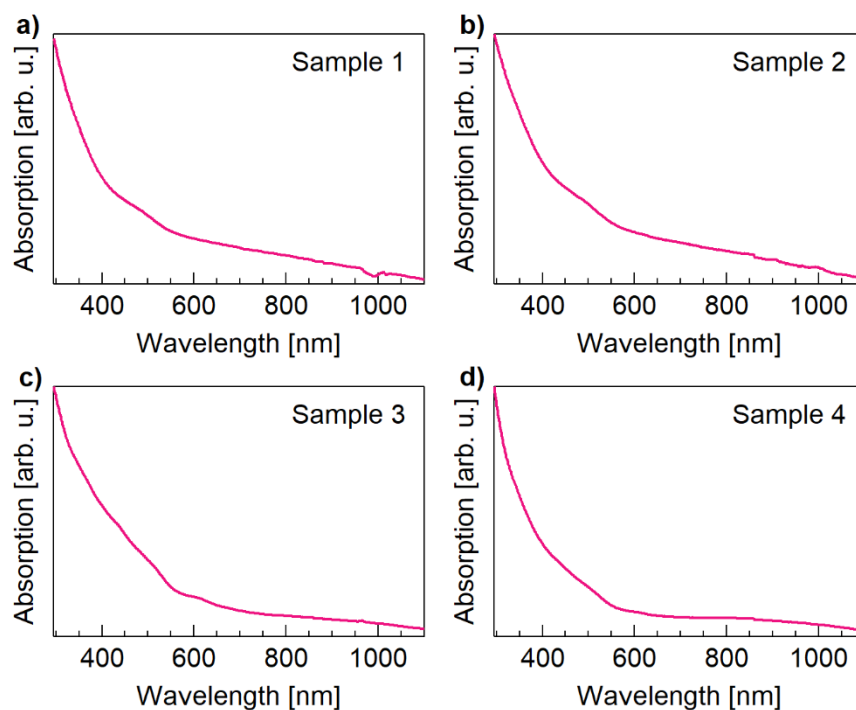
<sup>a</sup>Ghent University, Department of Chemistry, Krijgslaan 281, 9000 Gent, Belgium

<sup>b</sup>CIC nanoGUNE, Tolsa Hirbidea 76, E-20018 Donostia-San Sebastian, Spain

<sup>c</sup>Istituto Italiano di Tecnologia, Via Morego 30, 16163 Genova, Italy

## Preliminary data on WS<sub>2</sub> synthesis

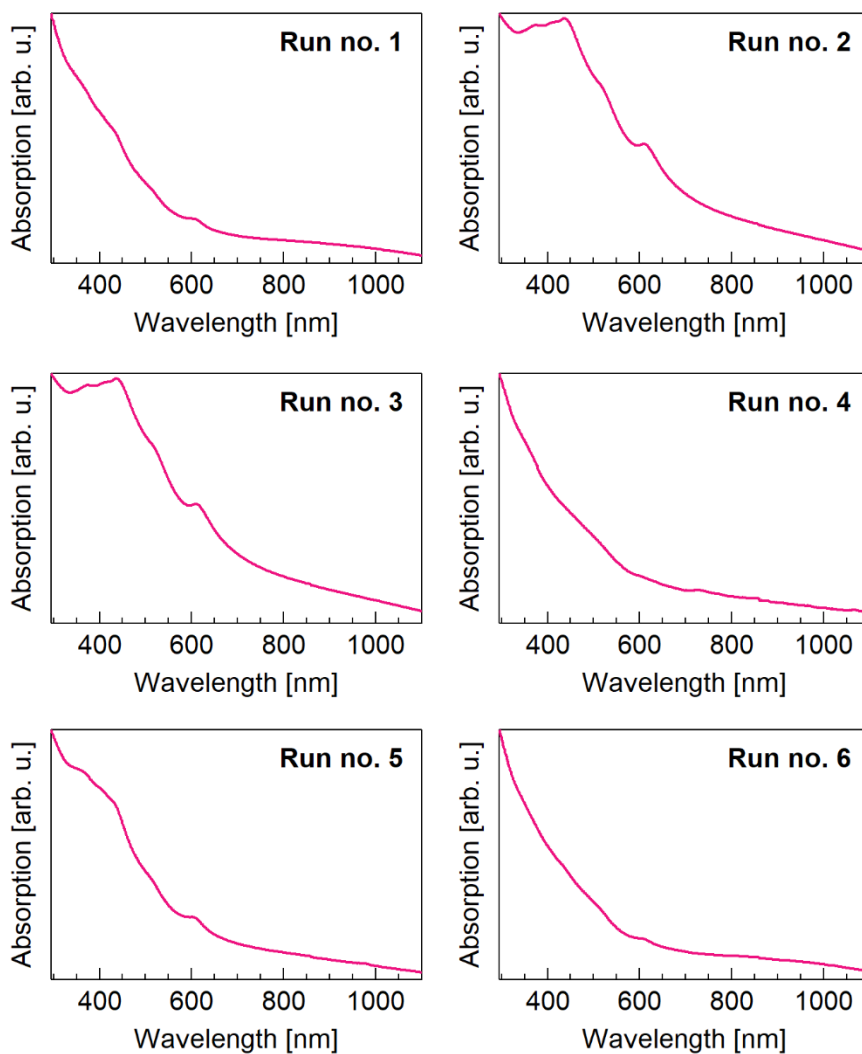
The factor ranges used in the DSD design are based on previous experimental work. To find a suitable range of values, we construct a DSD table and we then proceed to run the synthesis with the lowest factor values combination, since we hypothesize it would be the reaction that would most likely fail (*i.e.* resulting in the lack of measurable responses for the DSD framework). In **Figure S1** we report the UV-Vis absorption spectra of the preliminary data while in **Table S1** we report the factor values used in the synthesis.



**Figure S1.** Absorption spectra of sample 1 (a), sample 2 (b), sample 3 (c), and sample 4 (d) used to determine the factor ranges in the DSD framework.

**Table S1.** Input factor  $X_i$  ( $i = [1, 4]$ ) used in the preliminary experiments.  $X_1$  = Reaction temperature,  $X_2$  = Injection rate,  $X_3$  = S/W molecular ratio, and  $X_4$  = OA/W molecular ratio.

Sample no.	$X_1$ [°C]	$X_2$ [mL h <sup>-1</sup> ]	$X_3$	$X_4$	HMDS/W ratio
<b>1</b>	300	12	2	2	2
<b>2</b>	310	12	2	2	2
<b>3</b>	310	2	8	30	20
<b>4</b>	310	8	4	10	20



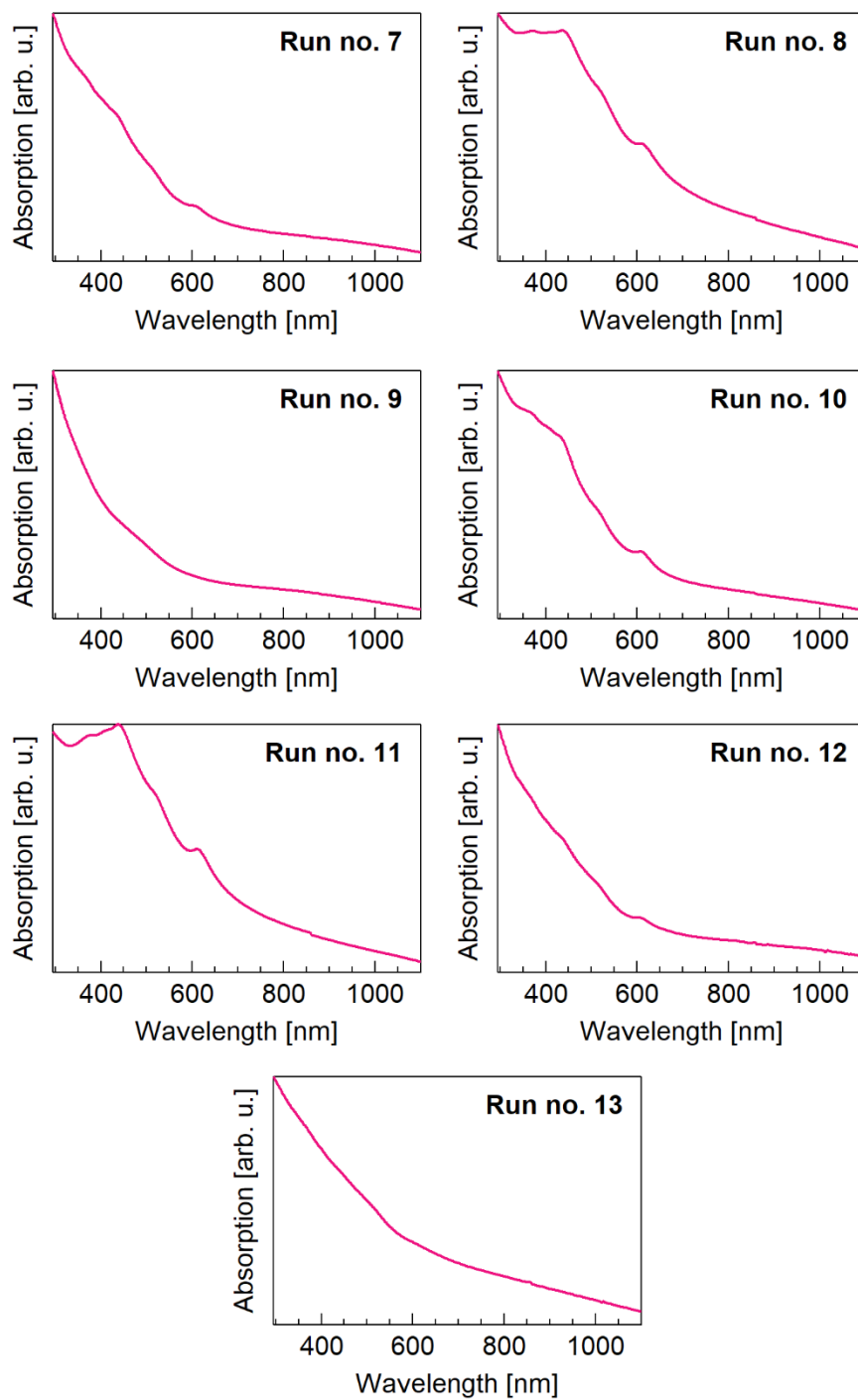


**Figure S2.** UV-Vis spectra of all the samples used in the DSD design.

## Design of Experiments – Definitive Screening Design on WS<sub>2</sub>

**General note.** In the DSD model, each response  $Y_i$  is fitted using a quadratic surface that involves linear as well as quadratic interactions between the input factors  $X_i$ ,  $X_i^2$ , and  $X_i \cdot X_j$ . In order to avoid model overfitting, we decided to minimize the Bayesian Information Criterion (BIC),<sup>1</sup> keeping at the same time a low corrected Akaike Information Criterion (AICc).<sup>2</sup> See references for further details.

**A exciton sharpness.** For the modelling, run no. 12 is discarded as it is identified as outlier. Such choice is made after correlating the residuals (calculated as the difference between the measured value and the predicted value) with the values of A exciton position predicted by the DSD model. Run no. 12 displays the highest residual among all runs (**Figure S3a**). A further check has been done using the studentized residuals (**Figure S3b**), calculated by dividing the residual by an estimate of its standard deviation; the standard deviation for each residual computed with the observation excluded. Such studentized value indicates how far (in standard deviation units) the single value (in this case the A exciton position) is from the average error. A value falling in the region delimited by the red lines (where the standard deviation distance from the average error is 4) is considered an outlier. Thus, run no. 12 A exciton value falls in the outlier region, and we excluded from the model.

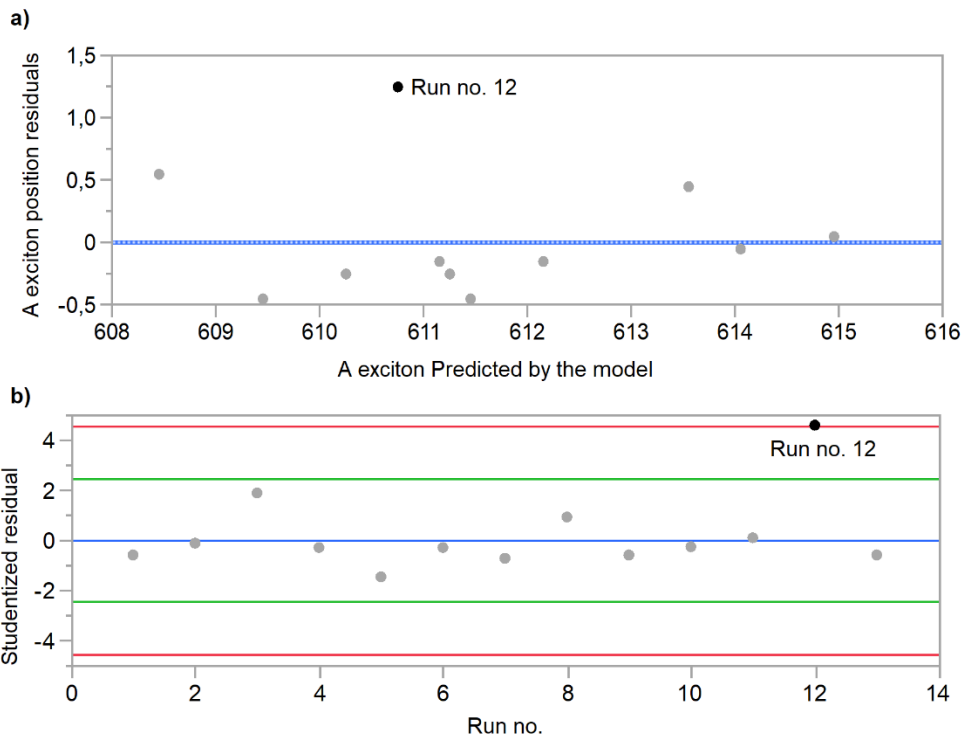


**Figure S3.** a) Correlation between the experimental residuals of the of A exciton position versus the values of A exciton position predicted by the DSD model. The blue line indicates a perfect match between experimental and predicted values, the dots represent each run result. b) Studentized residuals associated to each run. The red lines indicates the border region where a value is considered an outlier.

The model consists in a total of six factors, consisting in three main factors (injection rate, reaction temperature and S/W ratio), one two-factors interaction (reaction temperature · injection rate), and two quadratic interactions (reaction temperature · reaction temperature and S/W ratio · S/W ratio). The associated  $p$ -values are reported in **Table S2**.

**Table S2.** Factors interactions and relative  $p$ -values for A exciton sharpness model.

Factors		$p$ -values
X <sub>2</sub>	Injection rate	0.00010
X <sub>1</sub>	Reaction temperature	0.00083
X <sub>1</sub> · X <sub>2</sub>	Reaction temperature · Injection rate	0.00172
X <sub>3</sub>	S/W ratio	0.00210
X <sub>1</sub> · X <sub>1</sub>	Reaction T · Reaction T	0.03209
X <sub>3</sub> · X <sub>3</sub>	S/W · S/W	0.03560

**Background scattering.** For this analysis all runs are considered. We found a total of seven factors, featuring four main factor interactions (injection rate, reaction temperature, OA/W, S/W), two two-factor interaction (reaction temperature · OA/W and OA/W · S/W), and one quadratic interaction (OA/W · OA/W). The associated  $p$ -values are reported in **Table S3**.

**Table S3.** Factors interactions and relative  $p$ -value for background scattering model.

Factors		$p$ -values
X <sub>2</sub>	Injection rate	0.00002
X <sub>1</sub>	Reaction temperature	0.00006
X <sub>4</sub>	OA/W ratio	0.00015
X <sub>3</sub>	S/W ratio	0.00027
X <sub>4</sub> · X <sub>4</sub>	OA/W · OA/W	0.00367
X <sub>1</sub> · X <sub>4</sub>	Reaction T · OA/W	0.00473
X <sub>4</sub> · X <sub>3</sub>	OA/W · S/W	0.01122

### Nanosheet size- comparison between optimized samples and run no.11.

In **Figure S4** we report the HR-TEM images of A exciton, background optimized and the bright-field TEM images of run no. 11. Panels a-c are display the HR-TEM of the A exciton optimized sample, while panels d-f display the HR-TEM images of the background optimized sample. both samples show similar nanosheet morphology, with the visible edges of the nanosheet having an average length of 17 nm and standard deviation of 8 nm for the A exciton optimized sample and an average length of 16 nm and standard deviation of 7 nm for the background optimized sample. A comparison with run no. 11 sample (which displays a red shifted exciton position compared to the optimized samples, panels g-i) reveal nanoflower morphology and a larger average size (~50 nm).

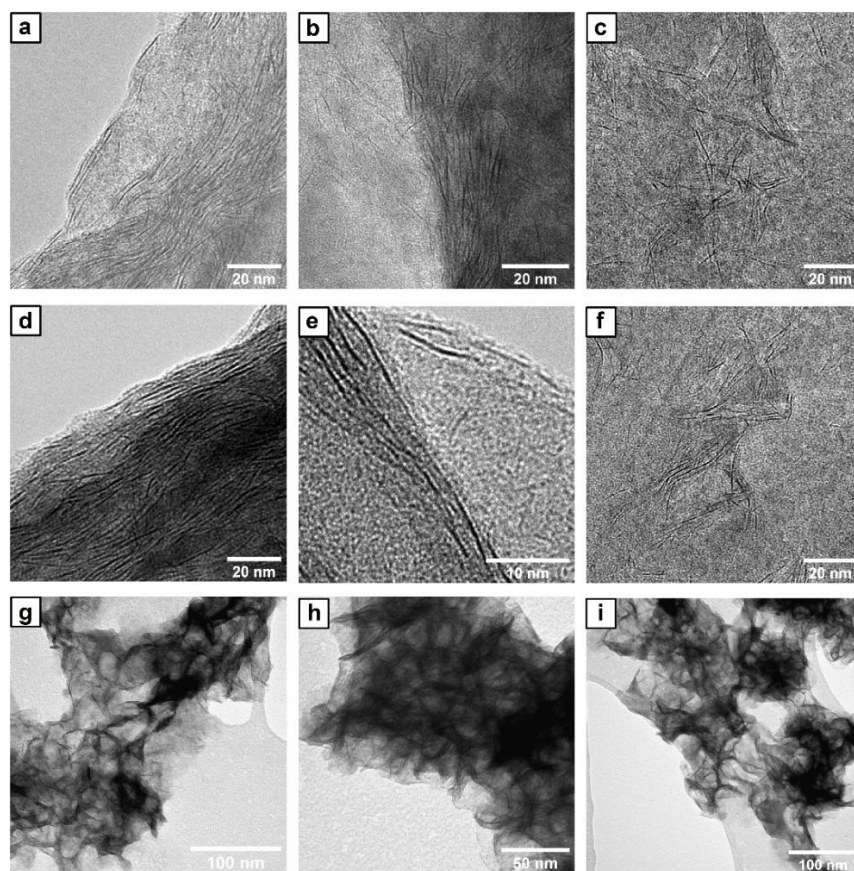


**Figure S4.** HR-TEM images of A exciton position optimized WS<sub>2</sub> sample (a-c), background optimized WS<sub>2</sub> sample (d-f) and run no. 11 (g-i) as comparison.



**A exciton optimized and background optimized sample nanosheet length distribution.**

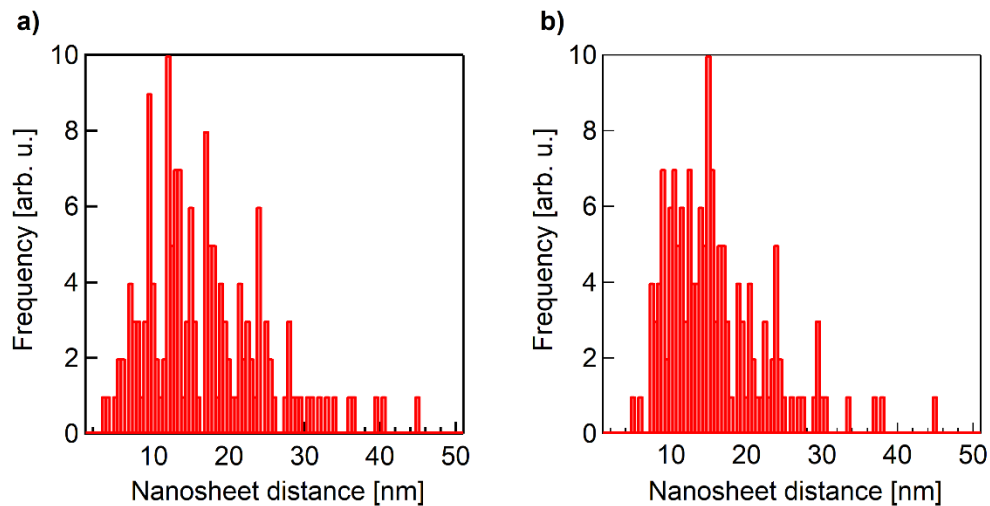


**Figure S5.** Histogram of the of A exciton position optimized WS<sub>2</sub> sample (a) and background optimized WS<sub>2</sub> sample (b) nanosheet length distribution.

**Nanosheet distance distribution for A exciton optimized and background optimized samples.**

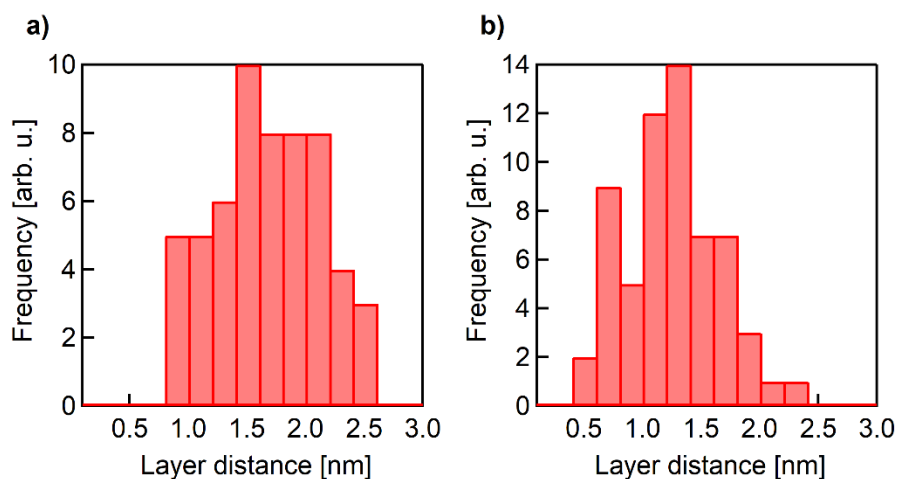


**Figure S6.** Histogram of the of A exciton position optimized WS<sub>2</sub> sample (a) and background optimized WS<sub>2</sub> sample (b) nanosheet distance distribution.

**PXRD of A exciton and background optimized samples.**

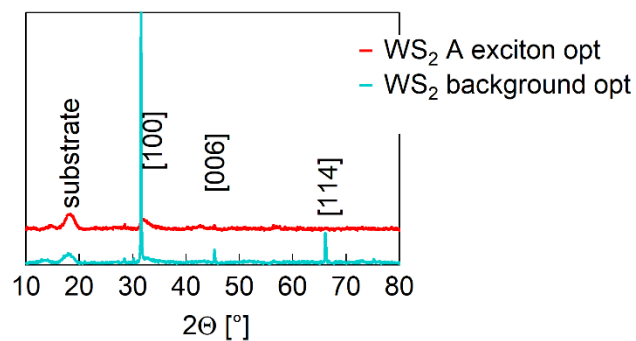


**Figure S7.** PXR D of A exciton and background optimized samples with assigned reflection (ICDS collection code 202366). The absence of the [002] reflection confirms the monolayer assignment to the samples.

## REFERENCES

1. Neath, A. A.; Cavanaugh, J. E., The Bayesian information criterion: background, derivation, and applications. *WIREs Computational Statistics* **2011**, *4* (2), 199-203.
2. Hurvich, C. M.; Tsai, C. L., Regression and Time-Series Model Selection in Small Samples. *Biometrika* **1989**, *76* (2), 297-307.